Science of the Total Environment 858 (2023) 159948

Contents lists available at ScienceDirect

Science of the Total Environment

journal homepage: www.elsevier.com/locate/scitotenv

$PM_{2.5}$ source apportionment identified with total and soluble elements in positive matrix factorization

Wenshuai Li [a,b], Yuxuan Qi [a,b], Wen Qu [c], Wenjun Qu [a,b], Jinhui Shi [d], Daizhou Zhang [e], Yingchen Liu [a,b], Yanjing Zhang [a,b], Weihang Zhang [a,b], Danyang Ren [a,b], Yuanyuan Ma [a,b], Xinfeng Wang [f], Li Yi [a,b], Lifang Sheng [a,b,*], Yang Zhou [a,b,*]

[a] Frontier Science Center for Deep Ocean Multispheres and Earth System (FDOMES) and Physical Oceanography Laboratory, Ocean University of China, Qingdao, Shandong, China
[b] College of Oceanic and Atmospheric Sciences, Ocean University of China, Qingdao, Shandong, China
[c] North China Sea Marine Forecasting Center of State Ocean Administration, Qingdao, Shandong, China
[d] College of Environmental Science and Engineering, Ocean University of China, Qingdao, Shandong, China
[e] Faculty of Environmental and Symbiotic Sciences, Prefectural University of Kumamoto, Kumamoto 862-8502, Japan
[f] Environment Research Institute, Shandong University, Qingdao, Shandong, China

HIGHLIGHTS

- The addition of soluble elements enables PMF to identify fresh and aged dust.
- Fly ash and aged pollutants from industrial sources could be distinguished by PMF involving soluble elements.
- The optimized PMF results will not significantly affect the factors analyzed by previous data sets.

GRAPHICAL ABSTRACT

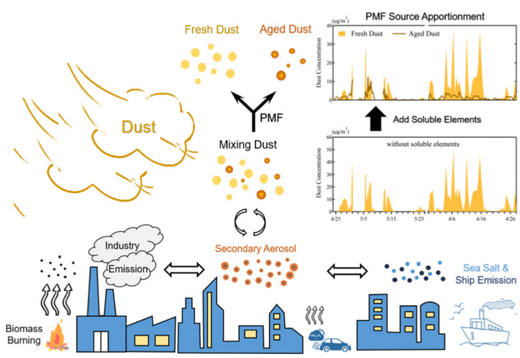

ARTICLE INFO

Editor: Philip K. Hopke

Keywords:
PMF
Aerosols
Soluble elements
Source apportionment
Composition data set

ABSTRACT

Source apportionments of urban aerosols identified with positive matrix factorization (PMF) are sensitive to input variables. So far, total elements were frequently included as effective factors in PMF-based source apportionment. We investigated the advances to involve soluble parts of elements in the source apportionment with four data sets of $PM_{2.5}$ composition observed at a coastal city (Qingdao) in northern China: water-soluble ions plus organic and elemental carbon (IC set), the IC set plus total elements (ICTE set), the IC set plus soluble elements (ICSE set), and the IC set plus both total elements and soluble elements (ICAE set). The apportionments of six sources, including secondary sulfate, secondary nitrate, secondary oxalate, sea salt, biomass burning and dust, were identified with the IC set. In comparison, pollutants from vehicle + coal combustion, ship emissions, waste incineration and industrial activities were also identified with the ICTE, ICSE, or ICAE sets. We found that the PMF solutions of the ICAE set could distinguish aged and fresh dust, and identify fly ash and aged pollutants from industrial sources. The profiles and corresponding time series of vehicle + coal combustion, secondary aerosols, ship emissions, sea salt, and biomass burning emissions identified with the four data sets were very similar, while discrepancies were encountered for waste incineration, dust, and industrial sources. These results indicate the benefits and potentials with total and soluble elements involved in PMF-based source apportionments.

* Corresponding authors at: College of Oceanic and Atmospheric Sciences, Ocean University of China, Qingdao, Shandong, China.
E-mail addresses: shenglf@ouc.edu.cn (L. Sheng), yangzhou@ouc.edu.cn (Y. Zhou).

http://dx.doi.org/10.1016/j.scitotenv.2022.159948
Received 10 June 2022; Received in revised form 19 October 2022; Accepted 31 October 2022
Available online 3 November 2022
0048-9697/© 2022 Published by Elsevier B.V.

1. Introduction

Particulate air pollution, especially fine particulate matter (i.e., $PM_{2.5}$) pollution, poses an enormous challenge due to its profound impacts on public health and the ecological environment (Brunekreef and Holgate, 2002; Lippmann and Chen, 2009). Identifying aerosol sources and determining the corresponding quantitative apportionment of $PM_{2.5}$ are fundamental aspects of studying the atmospheric environment. Receptor models (Chan et al., 2011), such as positive matrix factorization (PMF), are extensively used in the source apportionment of atmospheric particles (Bove et al., 2018; Lee et al., 2008; Manousakas et al., 2017).

Researchers always face a salient task to access the optimal PMF solution that determines which chemical species should be added as the input data. To date, various data sets of chemical species have been reported in PMF studies. The most commonly used data set comprises water-soluble ions (WSIs), elements, elemental carbon (EC), organic carbon (OC) and, sometimes, detailed organic tracers because these are the main components of aerosols and are representative of typical pollution sources (Bressi et al., 2014; Cesari et al., 2016; Dai et al., 2020; Lee et al., 2008; Uranishi et al., 2017). Other data sets, such as WSIs + elements (Duan et al., 2014; Lim et al., 2010; Tan et al., 2014), elements + black carbon (BC) (Cohen et al., 2010; Manousakas et al., 2017), and even elements only (Chang et al., 2018; Dall'Osto et al., 2013; Tian et al., 2018), have also been used to retrieve aerosol sources. In contrast, soluble elements have rarely been used in PMF studies owing to their relatively minor contributions (~4.8 % in this study) to the total element content. However, soluble elements can trace some specific pollution sources.

The sources of the soluble and insoluble fractions of a given element may differ. For instance, iron (Fe) is a crucial element in regulating oceanic primary productivity. Although the iron solubility in fresh mineral dust is usually comparatively low (Shi et al., 2012), it could be significantly enhanced after exposure to specific atmospheric processes (e.g., cloud process) (Hettiarachchi et al., 2019; Shi et al., 2015; Takahashi et al., 2011). Thus, soluble elements may be used to retrieve unique sources that are difficult to determine by using the total elements. However, few researchers have used soluble elements in PMF studies (Xie et al., 2012), and it remains unclear whether soluble elements can be successfully used in PMF-based source apportionment. Hence, in this work, we performed four PMF runs with different chemical species as the input data to study the potential role played by soluble elements in PMF-based source apportionment. We compared the PMF solutions of each chemical data set and considered the implications of using soluble elements in PMF-based source apportionment.

2. Materials and methods

2.1. Ambient sample collection

Qingdao is a coastal city located in northern China. It is a crucial monitoring site on the outlet transport route of Asian dust and heavily polluted air masses from the Beijing–Tianjin–Hebei (BTH) region to the Yellow Sea and the northwest Pacific Ocean. The sources of air pollution in spring are relatively complex, including both mineral dust sources and anthropogenic emissions. For studying the aging process of dust plumes during the long-range transport, aerosol observation was conducted at Baguanshan Atmospheric Research Observatory (BARO, 36°03′ N, 120°20′ E, ~76 m above sea level) in Qingdao during the periods April 24 to May 26 in 2017, March 28 to April 30 in 2018 and May 22 to May 28 in 2018. $PM_{2.5}$ samples were collected in the daytime (N = 70) and nighttime (N = 70). Sample collection time was 2.5–6 h, adjusted according to the weather conditions, e.g., sandstorms and haze conditions (Table S1). All the average results in this study are the time-weighted average. Two high-volume (~1.06 m^3/min) $PM_{2.5}$ samplers were utilized synchronously. One sampler used Quartz microfiber filters (QM-A, PALL) to detect the concentrations of WSIs (including K^+, Na^+, Mg^{2+}, Ca^{2+}, NH_4^+, Cl^-, SO_4^{2-}, NO_3^-, and $C_2O_4^{2-}$) and carbonaceous matter (OC and EC). The other sampler used Whatman® 41 filters to obtain samples for analyzing elements (Mg, Al, V, Cr, Mn, Fe, Ni, Cu, Zn, As, Se, Rb, Sr, Cd, Ba, and Pb). More details on measuring chemical species are provided in the Supplementary Material (Text S1).

2.2. Positive matrix factorization (PMF) and general input settings

The EPA PMF 5.0 model of the United States Environmental Protection Agency (EPA) was used to identify the primary sources of air pollutants. This is a receptor model for quantifying the contributions of different pollution sources based on the composition or fingerprints of the sources. To acquire robust results, we considered two uncertainty methods, which have been commonly used in previous research (Anttila et al., 1995; Polissar et al., 1998). Details are provided in Text S2. The results showed that the factor profiles of the PMF runs based on different uncertainty methods were very similar. Thus, the factor profile with a slightly smaller Q value (~8 %) was selected for discussion.

We compared the PMF results of four species data sets to investigate the impact of soluble elements on source apportionment. As shown in Table 1, the first data set (labeled "IC") only contained WSIs, OC and EC. The second data set (labeled "ICTE") comprised the IC set plus total elements. The third data set (labeled "ICSE") comprised the IC set plus soluble elements. The fourth data set (labeled "ICAE") combined the IC set with both total and soluble elements. The second, third, and fourth chemical data sets were collectively noted as the "CE" data sets as they all contained elements. We also considered replacing total elements with insoluble elements for the ICAE set. But total elements have more significant physical interpretability than insoluble elements, and there is no appropriate method to assess the uncertainties of insoluble elements directly. The factor number is another key aspect determining the optimal PMF solution. In this study, 3–8 factors were tested for the IC set, whereas 4–12 factors were tested for the CE sets. To certify the robustness of the statistics, 100 runs were performed for each calculation.

In addition, multiple F-peak values (between −1 and +1 in increments of 0.2) were explored to diminish the rotational ambiguity, thus obtaining more physically realistic solutions. Generally, the factor profile of the rotated results becomes more similar to the original factor profile as the F-peak value decreases. The solutions with F-peak values of −0.2 were chosen for all data sets by considering the lowest dQ values (within 0.7 % of the base run value) and the reasonability of factor profiles. The results of the PMF-based source apportionment for each data set are summarized in Table 1. More details about the PMF settings and outputs of the four data sets can be found in Texts S2–S3 and Tables S2–S6, respectively.

3. Results and discussion

As shown in Table 1, 6–10 factors were retrieved using PMF for the four data sets. The factor profiles of the CE and IC sets are shown in Figs. 1 and S1, respectively. The time series of factor concentrations for the CE sets are shown in Fig. S8. The factor contributions of ICTE and ICAE sets were shown in Fig. 2. The ICTE solution attributed more particle mass to biomass burning (BB) (20.0 %) and ship emissions (6.2 %), but less to secondary aerosols (10.9 %), compared with the results of the ICAE set (Fig. 2). It was mainly caused by the different contributions of dominant species in factors to the factor mass between the ICTE and ICAE sets (Fig. 1), which may result from the discrepancy of factor number, chemical species and rotational ambiguity during PMF calculation (Paatero et al., 2014). The factor contributions of the ICTE and ICAE sets were similar holistically ($P > 0.05$, variance analysis), indicating the robustness of the PMF results for these two data sets.

To examine the similarities of congeneric factors between different data sets, Pearson's correlation plots (Fig. 3) and PSCF (potential source contribution function) were implemented (Fig. S9). In general, many congeneric factors of the CE sets exhibited significant similarities with each other, including vehicle + coal combustion (VCC), secondary aerosols, sea salt (SS) and ship emissions. In contrast, considerable

Table 1
Summary of PMF solutions for each chemical data set (n = 140).

Data set	IC	ICTE	ICSE	ICAE
Input data	WSIs[a] + OCEC[b]	WSIs + OCEC + TE[c]	WSIs + OCEC + SE[d]	WSIs + OCEC + TE + SE
No. of input species	11	23	23	35
No. of factors	6	9	9	10
Factor 1	Secondary sulfate	Vehicle + coal combustion[e]	Vehicle + coal combustion	Vehicle + coal combustion
Factor 2	Secondary nitrate	Secondary aerosols[f]	Secondary aerosols	Secondary aerosols
Factor 3	Secondary oxalate	Ship emissions	Ship emissions	Ship emissions
Factor 4	Biomass burning	Biomass burning	Biomass burning	Biomass burning
Factor 5	Sea salt	Sea salt	Sea salt	Sea salt
Factor 6	General dust[g]	General dust	General dust	Fresh dust
Factor 7		Fresh dust[h]	Aged dust[i]	Aged dust
Factor 8		Waste incineration	Waste incineration	Waste incineration
Factor 9		Industry	Industry	Aged industrial sources[j]
Factor 10				Fly ash

[a] Water-soluble ions.
[b] Carbonaceous matter (OC and EC).
[c] Total elements.
[d] Soluble elements.
[e] The factor is dominated by NO_3^-, SO_4^{2-}, NH_4^+ and some anthropogenic elements.
[f] The factor is dominated by $C_2O_4^{2-}$, SO_4^{2-} and NH_4^+.
[g] The general dust factor is characterized by high abundances of K^+, Ca^{2+}, Mg^{2+}, and Cl^-.
[h] The fresh dust factor is characterized by high abundances of Ca^{2+}, total Al, Mn, Fe, Ba, Ni, Cu, As, and Cr.
[i] The aged dust factor is characterized by high abundances of soluble Al, Mn, Fe, and Ba.
[j] Aged pollutants from industrial sources: aged industrial sources (AIS).

discrepancies were observed for BB, dust, industrial sources and waste incineration.

3.1. Vehicle, coal combustion and secondary aerosols

For the 6-factor PMF results of the IC set, three factors were related to secondary aerosols (Fig. S1): secondary nitrate (SNT), secondary sulfate (SSF), and secondary oxalate (SOL), which are characterized by the prominence of nitrate, sulfate, and oxalate, respectively. For the CE sets, two factors were related to secondary aerosols, i.e., the VCC and the secondary aerosols (Fig. 1a and b). The VCC factors, were identified by the prominence of sulfate, nitrate, and ammonia (collectively referred to as "SNA"), as well as the noticeable contributions to Cu, As, Cd and Pb. Similar results have been obtained in previous studies, whereby sulfate and nitrate could undergo secondary formation in similar processes (Lim et al., 2010; Liu et al., 2016; Liu et al., 2014; Tan et al., 2014; Tian et al., 2020). Sulfate and nitrate are usually formed via the oxidation of SO_2 and NO_x, which are typically emitted by coal combustion and vehicle (Huang et al., 2014; Liu et al., 2020; Wang et al., 2020). Because of the presence of Cu, As, Cd and Pb, we attribute this factor as "vehicle + coal combustion" (Chang et al., 2018; Johansson et al., 2009; Peña-Fernández et al., 2015; Tian et al., 2015). There were probably some primary sulfate from coal combustion (Dai et al., 2019; Ding et al., 2021). Unfortunately, it is impossible to distinguish primary and secondary sulfate even with the latest PMF models. Extra indexes are necessary.

The secondary aerosols factors of the CE sets were characterized by significant contributions to $C_2O_4^{2-}$ and high loadings of SO_4^{2-} and NH_4^+. Oxalate can be primarily emitted by BB and secondarily produced through liquid-phase reactions (Meng et al., 2013; Yamasoe et al., 2000). Similar to previous studies, we found significant correlations between oxalate and sulfate (Fig. S6c), indicating a similar formation pathway (Carlton et al., 2007; Martinelango et al., 2007; Yao et al., 2002). Thus, this factor was also noted as a multiphase processes factor.

For different CE sets, the factor profiles and PSCF results of the VCC factors and the secondary aerosols factors were very similar (Figs. 1a, b, S9a3–S9a5 and S9b2–S9b4). Significant correlations (r = 0.70–0.97, Fig. 3a and b) and highly similar PSCF results (Fig. S9a1–S9b4) indicated that the different chemical data sets could identify the VCC and secondary aerosols well. The PSCF patterns indicate that their sources were mainly at the southwest or south of Qingdao in east China.

3.2. Sea salt and ship emissions

Ship emissions and SS are two marine source factors. As shown in Figs. 1c, d, and S1, the SS factor was identified by high loadings of Na^+, Cl^-, and Mg^{2+} (Nguyen et al., 2013). The ship emission factor made high contributions to V and Ni and was characterized by high SO_4^{2-} concentrations (Fridell et al., 2008). The diagnostic V/Ni (total state) mass ratios of the ICTE and ICAE sets were 3.08 and 3.05, respectively, which are similar to the results obtained in previous studies (Wang et al., 2019; Zhao et al., 2013). In contrast, the soluble V/Ni ratios of the ICSE and ICAE sets were 5.34 and 5.56, respectively. Significant correlations were observed for the time series of SS and ship emission factors between the PMF results of different data sets (r > 0.90, Figs. 3c, d, and S10), indicating the ability and consistency of different data sets to retrieve these two factors.

3.3. Biomass burning and dust

The BB factor contributed significantly to OC, EC, and K^+ (Figs. 1e and S1). However, few Cl^- was accounted for by the BB factor. We attributed the low Cl^- to the aging process of BB aerosols during transport when most Cl^- in biomass burning pollutants was titrated by HNO_3(g) and H_2SO_4(g) (Li et al., 2003; Zauscher et al., 2013). Significant correlations were found between the BB factors of the IC, ICTE, and ICSE sets (r = 0.81–0.93, Figs. 3e and S10). However, the mineral species Mg^{2+} and Ca^{2+} merged with the BB factor in the ICAE set (Fig. 1e) so that the correlations of the BB factor between the ICAE set and other data sets were much lower (r = 0.37–0.75).

The dust factor of the IC set was identified by the prominence of Mg^{2+} and Ca^{2+} and moderate loadings of K^+ and Cl^-. The CE sets obtained two dust factors for each data set, and three categories of dust factors could be classified (Table 2). The first category of the dust factor was characterized by the highest loadings of Mg^{2+} and Ca^{2+} (Fig. 1f), which were named "General Dust" in the ICTE and ICSE sets, resembling the dust factor of the IC set (r = 0.96–0.99). In contrast, the analogous dust factor merged with the BB factor in the ICAE set and had high factor loading values for Mg^{2+} and Ca^{2+}. Therefore, the BB factor PSCF result of the ICAE set resembled the PSCF results of the general dust factors, which mainly came from north China (Fig. S9e4, S9g1–S9g3). In this study, dust events were usually captured with the observations of fire spots on the transport pathways of dust plumes (Fig. S11). Therefore, K^+, OC and EC were highly correlated

Fig. 1. PMF factor profiles of the ICAE, ICTE, and ICSE sets. The concentration bar corresponds to the left y-axis, which is a logarithmic scale. The percentages of species correspond to the right y-axis. The letters "T" and "S" in the brackets behind element names refer to total and soluble elements, respectively.

with Mg^{2+} and Ca^{2+} during the dust period ($r = 0.77$–0.94). The PSCF results also suggested similar sources of these four compounds (Fig. S12), and the sources of the BB factors are mainly distributed on the pathways of dust plumes in north China.

The second category of dust factors made distinguishable contributions to water-soluble Ca^{2+} and total mineral elements (i.e., Al, Mn, Fe, and Ba, Fig. 1g) with low factor loadings for sulfate/nitrate and soluble metals, indicating a "fresh dust" factor for the ICTE and ICAE sets (Table 2). In

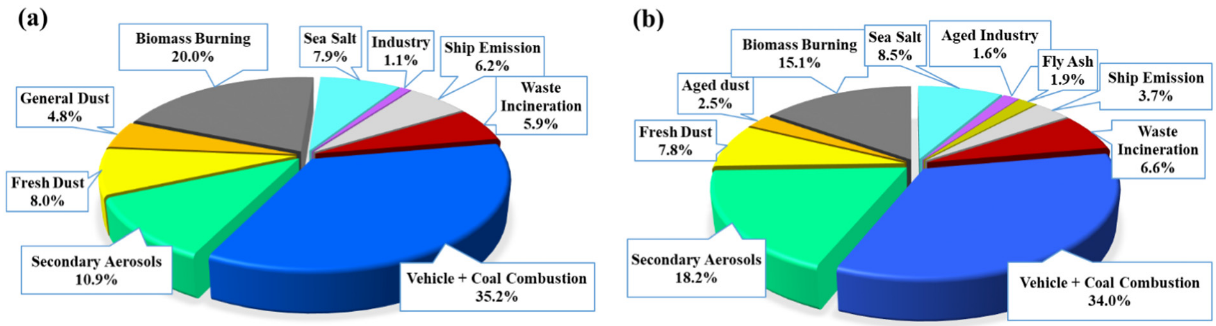

Fig. 2. Average of $PM_{2.5}$ contributions by each factor for the (a) ICTE and (b) ICAE sets.

comparison, the third category of dust factors was characterized by a high abundance of soluble mineral elements and some sulfate and nitrate (Fig. 1h and Table 2). Thus, it was termed the "aged dust" factor (Arimoto et al., 2004; Geng et al., 2014). In contrast to the fresh dust factor of the ICAE set, the aged dust factor contained a low percentage of total mineral elements but explained the conspicuous fractions of soluble elements. For the fresh dust factor, a significant correlation was observed between the ICTE and ICAE sets (r = 0.96). In contrast, for the aged dust factor, a significant correlation was observed between the ICSE and ICAE sets (r = 0.86). Moreover, the maximum concentration of the aged dust factor lagged that of the fresh dust factor during the dust event with a long duration (Fig. S13), indicating a reasonable dust aging process.

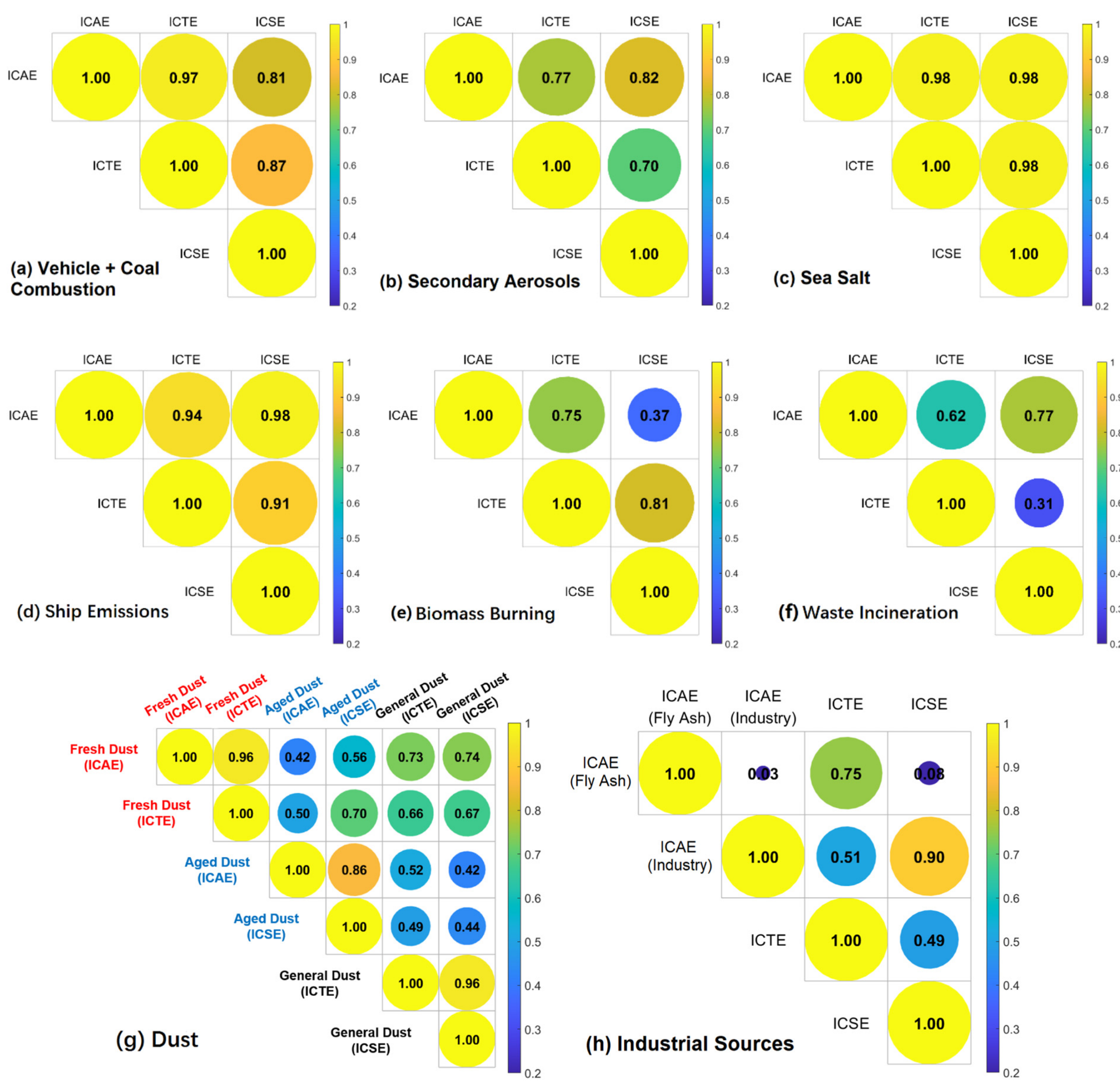

Fig. 3. Pearson's correlation coefficients between the same factors resulted from different PMF data sets.

Table 2
Summary of three categories of dust factors.

	Category I	Category II	Category III
Dominant species	K^+, Ca^{2+}, Mg^{2+}, and Cl^-	Ca^{2+}, total Al, Mn, Fe, Ba, Ni, Cu, As, and Cr	Soluble Al, Mn, Fe, and Ba
Factor	General dust (IC, ICTE, and ICSE sets)	Fresh dust (ICTE and ICAE sets)	Aged dust (ICSE and ICAE sets)

Positive correlations (r = 0.42–0.70) were also observed between the fresh dust (category II) and aged dust factors (category III), and the general dust factor (category I) was more strongly correlated with the fresh dust factor than the aged dust factor (Figs. 3g and S10). Nevertheless, we assumed that the fresh dust factor retrieved by the ICAE set was more reasonable because much more typical crustal tracers (i.e., Al, Mn, Fe, and Ba) were considered in the ICAE set. Details of the outputs of the two dust factors in the ICTE and ICSE sets were unclear, possibly due to the different analysis techniques used for WSIs and elemental species.

3.4. Industrial factors

Two categories of the industrial source factor were identified. One category had remarkable contributions to total anthropogenic elements (i.e., Cu, Zn, Cd, and Pb, see Fig. 1i), including the industry factor of the ICTE set and the fly ash factor of the ICAE set. The correlation between these contributions was 0.75 (Fig. 3h). The other category had significant contributions to soluble anthropogenic elements (Fig. 1j), including the industry factor of the ICSE set and the aged industrial sources factor of the ICAE set with a significant correlation (r = 0.90) and a high similarity of PSCF results between them (Figs. 3h, S9h2 and S9h4). Considering the interpretability of the industrial factors, we named the fly ash and aged industrial sources in the ICAE set.

Total Al and total Fe were the major chemical constituents of the fly ash factor (Deonarine et al., 2015; Belviso et al., 2015). The distinctive characteristic of fly ash is that the solubilities of its anthropogenic components (Ni, Cu, Zn, Cd, Pb, and Cr), defined as the ratios of their soluble contents to total contents, were very low (0–8.1 %, Table S7) (Belviso et al., 2015; Deonarine et al., 2015; Markowski and Filby, 1985). The fly ash factor had a distinctive PSCF pattern (Fig. S9h3) compared with the industry factors of the ICTE and ICSE sets (Fig. S9h1 and S9h2), indicating the limitation of PMF source apportionment with only total or soluble elements. The fly ash mainly originated from the northeast and southwest of Qingdao. In contrast, the dominant species in the aged industrial source factors of the ICAE set were soluble anthropogenic elements. Industrial pollutants can efficiently produce large amounts of soluble anthropogenic elements via atmospheric processing (Liu et al., 2022). This understanding is also supported by the fact that the correlations between total anthropogenic elements and SNA (r = 0.00–0.60, Fig. S14) were lower than those between soluble anthropogenic elements and SNA (r = 0.20–0.77, Fig. S15). Fig. S9h shows that industrial sources are mainly distributed in the south of Qingdao in East China, whose air pollutants likely underwent a remarkable aging process during the transport, considering that its similar PSCF pattern with that of the secondary aerosols' factors (Fig. S9a and S9b).

3.5. Waste incineration

As shown in Fig. 1k, the waste incineration factor usually contributed highly to Zn, Cu, and Cl^- (Font et al., 2015; Hu et al., 2003; Setyan et al., 2017; Wang et al., 2017). However, the waste incineration factor of the ICSE set contributed less to Cl^- than the corresponding factors of the ICTE and ICAE sets, and showed moderate correlations with those of the ICAE set (r = 0.77) and the ICTE set (r = 0.31), suggesting that the waste incineration factors retrieved by different data sets varied remarkably. Unfortunately, we do not have enough data for a proper evaluation of the stability of waste incineration factors because municipal wastes can vary temporally and spatially (Font et al., 2015; Hu et al., 2003; Wang et al., 2017). The low Cl^- in the ICSE set suggests a more aged state of waste incineration emissions, as the fresh one usually with abundant Cl^- and the aging of Cl^--containing aerosols caused by sulfate and nitrate formation usually results in the Cl^- depletion (Liu et al., 2018; Setyan et al., 2017). The ICTE set, as a classic chemical species data set, had a similar PSCF result and similar contributions of waste incineration to $PM_{2.5}$ as the ICAE set (Figs. 2, S9f1 and S9f3), suggesting that the waste incineration factors of the ICTE and ICAE sets were relatively reliable in terms of physical interpretability. In contrast, the PSCF result of the waste incineration factor with the ICSE set shows a distinctive pattern, revealing the deficiency of using soluble elements only in PMF-based anthropogenic source apportionment.

4. Conclusion

In this work, four PMF solutions were compared with the data sets of ions + OCEC (IC), ions + OCEC + total elements (ICTE), ions + OCEC + soluble elements (ICSE), and ions + OCEC + total elements + soluble elements (ICAE). All data sets can retrieve secondary aerosols, sea salt, dust and biomass burning. The data sets with elements (CE sets) additionally identified ship emission, waste incineration and industrial sources.

Our results demonstrated the robustness of the IC set in retrieving general air pollution sources. Compared with the IC set, the CE sets have the advantage of retrieving anthropogenic sources for more chemical species, because these added elements are more specific and stable tracers than water-soluble ions. For the ICAE set, more specific factors (i.e., fresh dust, aged dust, fly ash and aged industrial sources) were figured out with the input of both total and soluble elements. Therefore, more details of the potential sources and formation mechanisms of soluble elements and the aging process in dust plumes can be explored, which is essential to recognize the influence of dust transport on the marine ecosystem.

Our work shows the merits in the source apportionment of aerosols by inputting both total and soluble elements into the PMF model. To improve the accuracy in further studies, the influence of the discrepancy in analysis techniques used for water-soluble ions, total and soluble elements needs to be addressed. The limited ability of PMF to distinguish specific sources of air pollutants should also be carefully considered.

CRediT authorship contribution statement

Wenshuai Li: Methodology, Writing – original draft. **Yuxuan Qi:** Methodology, Data curation. **Wen Qu:** Methodology, Resources. **Wenjun Qu:** Methodology, Resources. **Jinhui Shi:** Methodology, Resources, Funding acquisition. **Daizhou Zhang:** Writing – review & editing. **Yingchen Liu:** Methodology, Resources. **Yanjing Zhang:** Methodology. **Weihang Zhang:** Methodology. **Danyang Ren:** Methodology. **Yuanyuan Ma:** Methodology. **Xinfeng Wang:** Methodology, Resources. **Li Yi:** Methodology, Resources. **Lifang Sheng:** Supervision, Writing – review & editing. **Yang Zhou:** Methodology, Supervision, Writing – review & editing, Project administration, Funding acquisition.

Data availability

Data will be made available on request.

Declaration of competing interest

The authors declare that they have no known competing financial interests or personal relationships that could have appeared to influence the work reported in this paper.

Acknowledgment

This research was supported by National Natural Science Foundation of China (Grant Number: 41875155, 41876131), National Key Research and Development Program of China (Grant Number: 2019YFA0607004) and National Natural Science Foundation of China (Grant Number: 41605114).

Appendix A. Supplementary data

Detection information of chemical species (Text S1); PMF operation related materials (Texts S2–S3); Table S1 showed the sampling duration details; Tables S2–S6 were used to illustrate the rationality of the PMF solutions; Factor profiles of the IC and CE sets (Figs. S1–S4) and time series of the normalized concentrations of PMF factors (Fig. S8); Pearson correlations between same type factors of different chemical data sets (Fig. S10); Texts S4–S5 and Figs. S5–S7 and S9 discussed the potential sources of chemical species; Time series of PM_{10}, normalized concentrations of fresh dust factors and aged dust factors during two dust events in 2017 and 2018 (Fig. S13); Correlations between elements (Cu, Zn, Cd, As, Pb, Cr) and SNA (sulfate, nitrate and ammonium) (Figs. S14–S15); Elements solubility of the aged industrial sources (AIS) factor and the fly ash factor of the ICAE set (Table S7). Supplementary data to this article can be found online at https://doi.org/10.1016/j.scitotenv.2022.159948.

References

Anttila, P., Paatero, P., Tapper, U., Järvinen, O., 1995. Source identification of bulk wet deposition in Finland by positive matrix factorization. Atmos. Environ. 29 (14), 1705–1718.
Arimoto, R., Zhang, X.Y., Huebert, B.J., Kang, C.H., Savoie, D.L., Prospero, J.M., Sage, S.K., Schloesslin, C.A., Khaing, H.M., Oh, S.N., 2004. Chemical composition of atmospheric aerosols from zhenbeitai, China, and gosan, South Korea, during ACE-Asia. J. Phys. Chem. A 109 (D19).
Belviso, C., Cavalcante, F., Di Gennaro, S., Palma, A., Ragone, P., Fiore, S., 2015. Mobility of trace elements in fly ash and in zeolitised coal fly ash. Fuel 144, 369–379.
Bove, M.C., Massabò, D., Prati, P., 2018. PMF5.0 vs. CMB8.2: an inter-comparison study based on the new European SPECIEUROPE database. Atmos. Res. 201, 181–188.
Bressi, M., Sciare, J., Ghersi, V., Mihalopoulos, N., Petit, J.E., Nicolas, J.B., Moukhtar, S., Rosso, A., Féron, A., Bonnaire, N., Poulakis, E., Theodosi, C., 2014. Sources and geographical origins of fine aerosols in Paris (France). Atmos. Chem. Phys. 14 (16), 8813–8839.
Brunekreef, B., Holgate, S.T., 2002. Air pollution and health. Lancet 360 (9341), 1233–1242.
Carlton, A.G., Turpin, B.J., Altieri, K.E., Seitzinger, S., Reff, A., Lim, H.-J., Ervens, B., 2007. Atmospheric oxalic acid and SOA production from glyoxal: results of aqueous photooxidation experiments. Atmos. Environ. 41 (35), 7588–7602.
Cesari, D., Donateo, A., Conte, M., Contini, D., 2016. Inter-comparison of source apportionment of PM10 using PMF and CMB in three sites nearby an industrial area in Central Italy. Atmos. Res. 182, 282–293.
Chan, Y.-C., Hawas, O., Hawker, D., Vowles, P., Cohen, D.D., Stelcer, E., Simpson, R., Golding, G., Christensen, E., 2011. Using multiple type composition data and wind data in PMF analysis to apportion and locate sources of air pollutants. Atmos. Environ. 45 (2), 439–449.
Chang, Y., Huang, K., Xie, M., Deng, C., Zou, Z., Liu, S., Zhang, Y., 2018. First long-term and near real-time measurement of trace elements in China's urban atmosphere: temporal variability, source apportionment and precipitation effect. Atmos. Chem. Phys. 18 (16), 11793–11812.
Cohen, D.D., Crawford, J., Stelcer, E., Bac, V.T., 2010. Characterisation and source apportionment of fine particulate sources at Hanoi from 2001 to 2008. Atmos. Environ. 44 (3), 320–328.
Dai, Q., Bi, X., Song, W., Li, T., Liu, B., Ding, J., Xu, J., Song, C., Yang, N., Schulze, B.C., Zhang, Y., Feng, Y., Hopke, P.K., 2019. Residential coal combustion as a source of primary sulfate in Xi'an, China. Atmos. Environ 196, 66–76.
Dai, Q., Hopke, P.K., Bi, X., Feng, Y., 2020. Improving apportionment of PM2.5 using multisite PMF by constraining G-values with a prioriinformation. Sci. Total Environ. 736, 139657.
Dall'osto, M., Querol, X., Amato, F., Karanasiou, A., Lucarelli, F., Nava, S., Calzolai, G., Chiari, M., 2013. Hourly elemental concentrations in PM2.5 aerosols sampled simultaneously at urban background and road site during SAPUSS – diurnal variations and PMF receptor modelling. Atmos. Chem. Phys. 13 (8), 4375–4392.
Deonarine, A., Kolker, A., Doughten, M.W., 2015. Trace elements in coal ash. Fact Sheet 6. https://doi.org/10.3133/fs20153037.
Ding, X., Li, Q., Wu, D., Wang, X., Li, M., Wang, T., Wang, L., Chen, J., 2021. Direct observation of sulfate explosive growth in wet plumes emitted from typical coal-fired stationary sources. Geophys. Res. Lett. 48 (6), e2020GL092071.
Duan, J., Tan, J., Hao, J., Chai, F., 2014. Size distribution, characteristics and sources of heavy metals in haze episod in Beijing. J. Environ. Sci. 26 (1), 189–196.
Font, A., De Hoogh, K., Leal-Sanchez, M., Ashworth, D.C., Brown, R.J.C., Hansell, A.L., Fuller, G.W., 2015. Using metal ratios to detect emissions from municipal waste incinerators in ambient air pollution data. Atmos. Environ. 113, 177–186.
Fridell, E., Steen, E., Peterson, K., 2008. Primary particles in ship emissions. Atmos. Environ. 42 (6), 1160–1168.
Geng, H., Hwang, H., Liu, X., Dong, S., Ro, C.U., 2014. Investigation of aged aerosols in size-resolved asian dust storm particles transported from Beijing, China, to incheon, Korea, using low-Z particle EPMA. Atmos. Chem. Phys. 14 (7), 3307–3323.
Hettiarachchi, E., Reynolds, R.L., Goldstein, H.L., Moskowitz, B., Rubasinghege, G., 2019. Bioavailable iron production in airborne mineral dust: controls by chemical composition and solar flux. Atmos. Environ. 205, 90–102.
Hu, C.-W., Chao, M.-R., Wu, K.-Y., Chang-Chien, G.-P., Lee, W.-J., Chang, L.W., Lee, W.-S., 2003. Characterization of multiple airborne particulate metals in the surroundings of a municipal waste incinerator in Taiwan. Atmos. Environ. 37 (20), 2845–2852.
Huang, R.-J., Zhang, Y., Bozzetti, C., Ho, K.-F., Cao, J.-J., Han, Y., Daellenbach, K.R., Slowik, J.G., Platt, S.M., Canonaco, F., Zotter, P., Wolf, R., Pieber, S.M., Bruns, E.A., Crippa, M., Ciarelli, G., Piazzalunga, A., Schwikowski, M., Abbaszade, G., Schnelle-Kreis, J., Zimmermann, R., An, Z., Szidat, S., Baltensperger, U., Haddad, I.E., Prévôt, A.S.H., 2014. High secondary aerosol contribution to particulate pollution during haze events in China. Nature 514 (7521), 218–222.
Johansson, C., Norman, M., Burman, L., 2009. Road traffic emission factors for heavy metals. Atmos. Environ. 43 (31), 4681–4688.
Lee, S., Liu, W., Wang, Y., Russell, A.G., Edgerton, E.S., 2008. Source apportionment of PM2.5: comparing PMF and CMB results for four ambient monitoring sites in the southeastern United States. Atmos. Environ. 42 (18), 4126–4137.
Li, J., Posfai, M., Hobbs, P.V., Buseck, P.R., 2003. Individual aerosol particles from biomass burning in southern Africa: 2. Compositions and aging of inorganic particles. J. Geophys. Res. 108 (D13), 8484. https://doi.org/10.1029/2002JD002310.
Lim, J.-M., Lee, J.-H., Moon, J.-H., Chung, Y.-S., Kim, K.-H., 2010. Source apportionment of PM10 at a small industrial area using positive matrix factorization. Atmos. Res. 95 (1), 88–100.
Lippmann, M., Chen, L.-C., 2009. Health effects of concentrated ambient air particulate matter (CAPs) and its components. Crit. Rev. Toxicol. 39 (10), 865–913.
Liu, B., Song, N., Dai, Q., Mei, R., Sui, B., Bi, X., Feng, Y., 2016. Chemical composition and source apportionment of ambient PM2.5 during the non-heating period in Taian, China. Atmos. Res. 170, 23–33.
Liu, M., Wang, W., Li, J., Wang, T., Xu, Z., Song, Y., Zhang, W., Zhou, L., Lian, C., Yang, J., Li, Y., Sun, Y., Tong, S., Guo, Y., Ge, M., 2022. High fraction of soluble trace metals in fine particles under heavy haze in Central China. Sci. Total Environ. 841, 156771.
Liu, P., Ye, C., Xue, C., Zhang, C., Mu, Y., Sun, X., 2020. Formation mechanisms of atmospheric nitrate and sulfate during the winter haze pollution periods in Beijing: gas-phase, heterogeneous and aqueous-phase chemistry. Atmos. Chem. Phys. 20 (7), 4153–4165.
Liu, Q., Liu, Y., Yin, J., Zhang, M., Zhang, T., 2014. Chemical characteristics and source apportionment of PM10 during asian dust storm and non-dust storm days in Beijing. Atmos. Environ. 91, 85–94.
Liu, Y., Fan, Q., Chen, X., Zhao, J., Ling, Z., Hong, Y., Li, W., Chen, X., Wang, M., Wei, X., 2018. Modeling the impact of chlorine emissions from coal combustion and prescribed waste incineration on tropospheric ozone formation in China. Atmos. Chem. Phys. 18 (4), 2709–2724.
Manousakas, M., Papaefthymiou, H., Diapouli, E., Migliori, A., Karydas, A.G., Bogdanovic-Radovic, I., Eleftheriadis, K., 2017. Assessment of PM2.5 sources and their corresponding level of uncertainty in a coastal urban area using EPA PMF 5.0 enhanced diagnostics. Sci. Total Environ. 574, 155–164.
Markowski, G.R., Filby, R., 1985. Trace element concentration as a function of particle size in fly ash from a pulverized coal utility boiler. Environ. Sci. Technol. 19 (9), 796–804.
Martinelango, P.K., Dasgupta, P.K., Al-Horr, R.S., 2007. Atmospheric production of oxalic acid/oxalate and nitric acid/nitrate in the Tampa Bay airshed: parallel pathways. Atmos. Environ. 41 (20), 4258–4269.
Meng, J., Wang, G., Li, J., Cheng, C., Cao, J., 2013. Atmospheric oxalic acid and related secondary organic aerosols in Qinghai Lake, a continental background site in Tibet plateau. Atmos. Environ. 79, 582–589.
Nguyen, Q.T., Skov, H., Sørensen, L.L., Jensen, B.J., Grube, A.G., Massling, A., Glasius, M., Nøjgaard, J.K., 2013. Source apportionment of particles at station Nord, north East Greenland during 2008–2010 using COPREM and PMF analysis. Atmos. Chem. Phys. 13 (1), 35–49.
Paatero, P., Eberly, S., Brown, S.G., Norris, G.A., 2014. Methods for estimating uncertainty in factor analytic solutions. Atmos. Meas. Tech. 7 (3), 781–797.
Peña-Fernández, A., Lobo-Bedmar, M.C., González-Muñoz, M.J., 2015. Annual and seasonal variability of metals and metalloids in urban and industrial soils in Alcalá de Henares (Spain). Environ. Res. 136, 40–46.
Polissar, A.V., Hopke, P.K., Malm, W.C., Sisler, J.F., 1998. Atmospheric aerosol over Alaska: 1. Spatial and seasonal variability. J. Phys. Chem. A 103 (D15), 19035–19044.
Setyan, A., Patrick, M., Wang, J., 2017. Very low emissions of airborne particulate pollutants measured from two municipal solid waste incineration plants in Switzerland. Atmos. Environ. 166, 99–109.
Shi, Z., Krom, M.D., Jickells, T.D., Bonneville, S., Carslaw, K.S., Mihalopoulos, N., Baker, A.R., Benning, L.G., 2012. Impacts on iron solubility in the mineral dust by processes in the source region and the atmosphere: a review. Aeolian Res. 5, 21–42.
Shi, Z.B., Krom, M.D., Bonneville, S., Benning, L.G., 2015. Atmospheric processing outside clouds increases soluble iron in mineral dust. Environ. Sci. Technol. 49 (3), 1472–1477.
Takahashi, Y., Higashi, M., Furukawa, T., Mitsunobu, S., 2011. Change of iron species and iron solubility in asian dust during the long-range transport from western China to Japan. Atmos. Chem. Phys. 11 (21), 11237–11252.
Tan, J.-H., Duan, J.-C., Ma, Y.-L., Yang, F.-M., Cheng, Y., He, K.-B., Yu, Y.-C., Wang, J.-W., 2014. Source of atmospheric heavy metals in winter in Foshan, China. Sci. Total Environ. 493, 262–270.
Tian, H., Zhu, C.Y., Gao, J.J., Cheng, K., Hao, J.M., Wang, K., Hua, S.B., Wang, Y., Zhou, J.R., 2015. Quantitative assessment of atmospheric emissions of toxic heavy metals from anthropogenic sources in China: historical trend, spatial distribution, uncertainties, and control policies. Atmos. Chem. Phys. 15 (17), 10127–10147.

Tian, S., Liang, T., Li, K., Wang, L., 2018. Source and path identification of metals pollution in a mining area by PMF and rare earth element patterns in road dust. Sci. Total Environ. 633, 958–966.

Tian, Y., Zhang, Y., Liang, Y., Niu, Z., Xue, Q., Feng, Y., 2020. PM2.5 source apportionment during severe haze episodes in a chinese megacity based on a 5-month period by using hourly species measurements: explore how to better conduct PMF during haze episodes. Atmos. Environ. 224, 117364.

Uranishi, K., Ikemori, F., Nakatsubo, R., Shimadera, H., Kondo, A., Kikutani, Y., Asano, K., Sugata, S., 2017. Identification of biased sectors in emission data using a combination of chemical transport model and receptor model. Atmos. Environ. 166, 166–181.

Wang, Q., Huang, X.H.H., Tam, F.C.V., Zhang, X., Liu, K.M., Yeung, C., Feng, Y., Cheng, Y.Y., Wong, Y.K., Ng, W.M., Wu, C., Zhang, Q., Zhang, T., Lau, N.T., Yuan, Z., Lau, A.K.H., Yu, J.Z., 2019. Source apportionment of fine particulate matter in Macao, China with and without organic tracers: a comparative study using positive matrix factorization. Atmos. Environ. 198, 183–193.

Wang, Y., Cheng, K., Wu, W., Tian, H., Yi, P., Zhi, G., Fan, J., Liu, S., 2017. Atmospheric emissions of typical toxic heavy metals from open burning of municipal solid waste in China. Atmos. Environ. 152, 6–15.

Wang, Y., Tang, G., Zhao, W., Yang, Y., Wang, L., Liu, Z., Wen, T., Cheng, M., Wang, Y., Wang, Y., 2020b. Different roles of nitrate and sulfate in air pollution episodes in the North China plain. Atmos. Environ. 224, 117325.

Xie, M., Hannigan, M.P., Dutton, S.J., Milford, J.B., Hemann, J.G., Miller, S.L., Schauer, J.J., Peel, J.L., Vedal, S., 2012. Positive matrix factorization of PM2.5: comparison and implications of using different speciation data sets. Environ. Sci. Technol. 46 (21), 11962–11970.

Yamasoe, M.A., Artaxo, P., Miguel, A.H., Allen, A.G., 2000. Chemical composition of aerosol particles from direct emissions of vegetation fires in the Amazon Basin: water-soluble species and trace elements. Atmos. Environ. 34 (10), 1641–1653.

Yao, X., Fang, M., Chan, C.K., 2002. Size distributions and formation of dicarboxylic acids in atmospheric particles. Atmos. Environ. 36 (13), 2099–2107.

Zauscher, M.D., Wang, Y., Moore, M.J.K., Gaston, C.J., Prather, K.A., 2013. Air quality impact and physicochemical aging of biomass burning aerosols during the 2007 San Diego wildfires. Environ. Sci. Technol. 47 (14), 7633–7643.

Zhao, M., Zhang, Y., Ma, W., Fu, Q., Yang, X., Li, C., Zhou, B., Yu, Q., Chen, L., 2013. Characteristics and ship traffic source identification of air pollutants in China's largest port. Atmos. Environ. 64, 277–286.